

Two-photon photocurrent imaging of vertical cavity surface emitting lasers

Chris Xu,^{a)} Leo M. F. Chirovsky, W. S. Hobson, J. Lopata, Wayne H. Knox, John E. Cunningham, William Y. Jan, and L. A. D'Asaro
Bell Laboratories, Lucent Technologies, Holmdel, New Jersey 07733

(Received 22 November 1999; accepted for publication 25 January 2000)

We show that two-photon photocurrent imaging can be used to nondestructively study vertical cavity surface emitting lasers on a microscopic level. In particular, we study the aperture isolation created by shallow ion implantation. The combination of two-photon backside imaging and a probe station is ideal for internal and full wafer characterization. The required peak and average power levels for testing can be easily satisfied by available compact ultrafast laser sources, making the technique practical and user friendly. © 2000 American Institute of Physics. [S0003-6951(00)03612-3]

Recently there has been intensive research on vertical cavity surface emitting lasers (VCSELs). Driven by a wide variety of applications in optical communications such as optical interconnects, high speed local area networks, optical signal processing, etc., VCSEL technology has made significant progress. Low threshold currents and voltages, as well as high output powers and external efficiencies have been reported. Creative design and processing steps are employed to improve device performance.¹⁻³ Thus far, VCSEL structures with the highest efficiencies have been devices with oxide-defined current apertures. However, VCSELs with implant-defined current apertures require only photolithographic processing steps. The basic theory of ion implantation is understood⁴ and ion implants have been used in VCSEL processing since the early 90's.⁵ These were deep implants (several microns) into the top mirror. Recently, the use of shallow implants has been introduced.⁶ The effectiveness of these implants is still a concern in regards to VCSEL performance and reliability.

To aide the VCSEL design and fabrication, we employ two-photon photocurrent testing method to quantitatively study VCSELs on a microscopic level. This study focuses mainly on the current aperture formation by the implantation process, an issue of critical importance to VCSEL performance. Similar to two-photon backside imaging of integrated circuits,^{7,8} two-photon excitation provides a convenient way of injecting localized carriers in the P-I-N diodes of the laser through the GaAs substrate. Because the photon energy of the excitation beam is below the substrate band gap, two-photon photocurrent generation circumvents the problem caused by the opacity of the substrate and the top metal layer. Backside illumination allows the use of ordinary microprobes to contact the VCSELs on the front side, without the restriction of the probe movement and the requirement of long working distance lenses. Thus, high numerical aperture objectives can be used to achieve high spatial resolution ($\leq 1 \mu\text{m}$). Furthermore, the technique requires no packaging, is nondestructive, and can be implemented as a wafer-scale tool.

The experimental layout is illustrated in Fig. 1. In es-

sence, the setup combines an inverted laser scanning microscope with a standard probe station. A compact modelocked fiber laser (Femtolite B-35, IMRA America) is used as the illumination source. The laser provides an average power of 40 mW and ≤ 300 fs pulses with ~ 48 MHz repetition rate at $1.55 \mu\text{m}$. The excitation beam was raster scanned by two galvanometer-driven mirrors (Cambridge Technology 6860) and focused by a microscope objective [either 100 X/0.85 numerical aperture, Hamamatsu A3717 or 100 X/0.9 infrared (IR), Zeiss]. Both objective lenses feature a correction collar for imaging through thick substrates. By carefully adjusting the collar, spherical aberration caused by the index mismatch of the air/substrate interface can be completely compensated. (Performance of the lenses are confirmed by measuring the axial response of confocal imaging.) The relay lenses between the scan mirrors and the objective also serve as a beam expander. The beam diameter at the back aperture of the objective lens is approximately 10 mm, large enough to achieve a diffraction limited focus at the sample. The backsides of the VCSEL wafers were chemical-mechanical polished to a mirror finish, the only sample preparation step

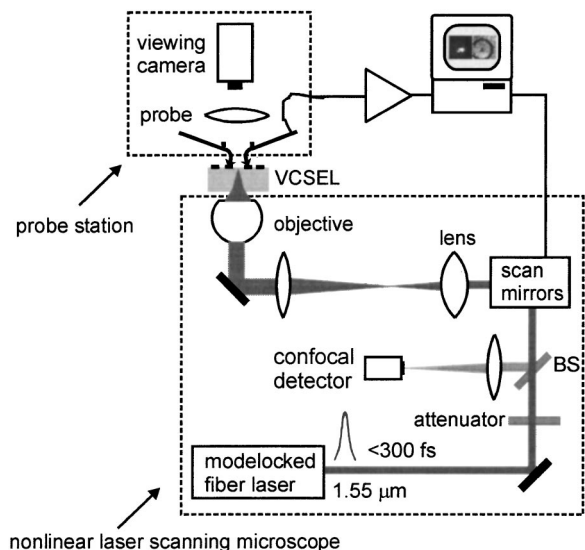


FIG. 1. Experimental setup for the two-photon photocurrent imaging of VCSELs.

^{a)}Electronic mail: chrisxu@lucent.com

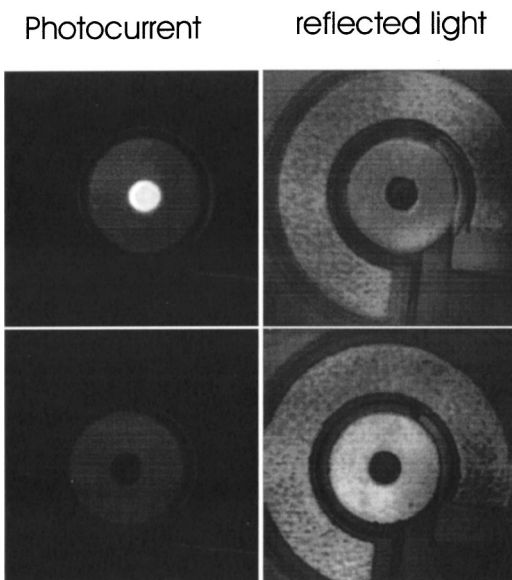


FIG. 2. Simultaneous two-photon photocurrent and confocal reflected light images of 980 VCSELs with implant-defined current aperture. The gray scales represent the photocurrent and reflected light levels. The top row shows a normal VCSEL and the bottom row shows a fully implanted test VCSEL. Top and bottom images were obtained under identical conditions. The size of the current aperture is $10\ \mu\text{m}$. See Ref. 6 for detailed VCSEL structure.

required before testing. Ordinary microprobes were used to contact the VCSELs. An IR sensitive camera was used to guide the probes and locate the incident beam. Two-photon generated current was recorded as a function of the beam position and displayed as photocurrent maps of the VCSELs. Although results reported here are for VCSELs under zero bias, images have also been taken for VCSELs under reverse bias, for example, to measure the spatial variations of the breakdown voltage. For comparison and registration purposes, confocal reflected light images are also obtained. The backreflected light is collected by the objective lens and descanned by the scan mirrors. An 8% reflection beam splitter is used to separate the reflection path from the excitation path. A 250 mm focal-length lens then focuses the light onto a fiber-coupled InGaAs photodiode (2011, Newfocus). The small area of the fiber input (diameter= $62.5\ \mu\text{m}$) is used as the confocal aperture. Average powers of less than 5 mW at the sample are typically used in our experiments. Detailed VCSEL structure and processing steps have been reported elsewhere.⁶

The effectiveness of the two-photon photocurrent method is demonstrated in Fig. 2. Two 980 VCSELs, one normal device with a $10\ \mu\text{m}$ current aperture and the other a test device with implant throughout the active layer, were imaged. While the confocal reflected light images showed virtually no difference, the contrast is apparent in the two-photon photocurrent images. Figure 3 compares quantitatively the photocurrent levels of a normal VCSEL and two fully implanted devices. Within the implant-defined current aperture, the photocurrent measured in the normal device is more than 15 times larger than that of the fully implanted devices, showing clearly the current-blocking effect of the implant process. Outside of the current aperture, the measured photocurrent levels are about the same for the normal and fully implanted devices, i.e., the large difference in con-

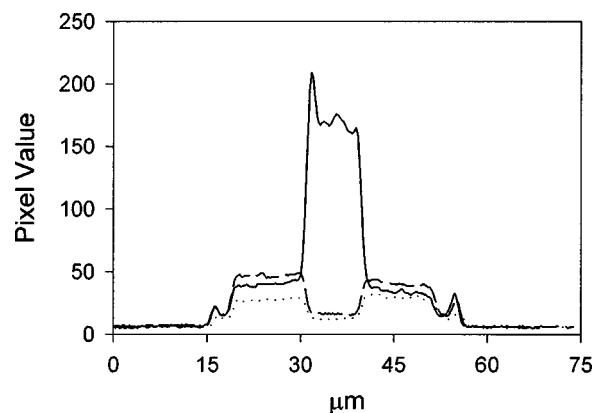


FIG. 3. Line plots of the photocurrent levels. The lines were taken through the middle of the $10\ \mu\text{m}$ current apertures. The solid line is data taken with a normal VCSEL. The dashed and dotted lines are data taken with two fully implanted devices. Pixel value of 150 represents photocurrent of $10\ \mu\text{A}$.

ductivity within the current aperture has no effect on the region outside. Combined with the observation of the sharp aperture boundary, we can conclude that lateral carrier diffusion is negligible in the detected photocurrent and the detected photocurrent represents the local property of the device. The devices shown in Figs. 2 and 3 are identical except for the implant layer. Thus, Figs. 2 and 3 also show that the two-photon photocurrent image represents the properties of the implant layer, despite the fact that free carriers are generated throughout the confocal length (about $6\ \mu\text{m}$ inside the substrate), which is much larger than the active layer of the VCSEL (less than $0.1\ \mu\text{m}$).⁶ Although only results for 980 nm VCSELs were reported here, we have also successfully used the same technique to study 850 nm VCSELs (results not shown).

The study of the failure mechanisms of VCSELs can also be aided by the two-photon photocurrent technique, particular in locating the defect sites. As an example, the VCSEL shown in Fig. 4 was intentionally subjected to ex-

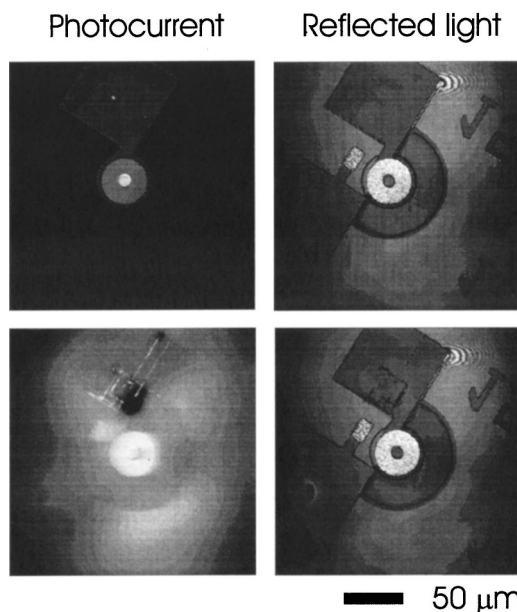


FIG. 4. Simultaneous two-photon photocurrent and confocal reflected light images of 980 VCSELs before (top) and after (bottom) operating at 24 mA for several minutes.

treme conditions (24 mA and 6 V, approximately $12\times$ threshold or $1.2\times$ rollover current level) in order to speed up the degradation process. The uniform degradation of the mesa, i.e., the lack of localized defects in the mesa region, is likely caused by the thermal annealing of the implant; while the localized breakdown at the P contact possibly indicates regions of high field strength. The degraded VCSEL still lased but only at about 20% of its normal power level. The bias voltage to achieve the same current also dropped significantly, consistent with the observation of a leaky aperture. We also note that the backside confocal reflected light images before and after degradation showed little difference, indicating no significant change in the optical properties of the device.

In summary, we have shown that two-photon photocurrent imaging can be used to quantitatively study VCSELs on a microscopic level. The combination of two-photon backside imaging and the probe station is well suited for internal and full wafer scale testing. The fact that the image is obtained through the backside of the devices makes the technique particularly useful for characterizing VCSELs designed for flip-chip bonding even before the removal of the

substrates. Finally, the required peak and average power levels for testing can be easily satisfied by the available compact ultrafast laser sources, making the technique practical and user friendly.

The authors gratefully acknowledge IMRA America for providing the laser. The authors also acknowledge valuable help from N. Bonadeo, M. Mitchell, and B. Collings.

¹T. E. Sale, *Vertical Cavity Surface Emitting Lasers* (Wiley, New York, 1995).

²T. P. Lee, *Current Trends in Vertical Cavity Surface Emitting Lasers* (Word Scientific, Singapore, 1995).

³C. Wilmsen, H. Temkin, and L. A. Coldren, *Vertical-Cavity Surface-Emitting Lasers* (Cambridge University Press, New York, 1999).

⁴D. C. D'Avanzo, *IEEE Trans. Electron Devices* **ED-29**, 1051 (1982).

⁵Y. H. Lee, B. Tell, K. Brown-Goebeler, J. L. Jewell, and J. V. Hove, *Electron. Lett.* **26**, 710 (1990).

⁶L. M. F. Chirovsky, W. S. Hobson, R. E. Leibenguth, S. P. Hui, J. Lopata, G. J. Zydzik, G. Giaretta, K. W. Goossen, J. D. Wynn, A. V. Krishnamoorthy, B. J. Tseng, J. M. Vandenberg, and L. A. D'Asaro, *IEEE Photonics Technol. Lett.* **11**, 500 (1999).

⁷C. Xu and W. Denk, *Appl. Phys. Lett.* **71**, 2578 (1997).

⁸C. Xu and W. Denk, *J. Appl. Phys.* **86**, 2226 (1999).